Proceedings of FEDSM'98
1998 ASME Fluids Engineering Division Summer Meeting
June 21-25, 1998 Washington, DC

FEDSM98-4829

APPLICATIONS OF THE WAVELET TRANSFORM TO THE METEOROLOGICAL VECTOR DATA

Sawa Matsuyama, Yuko Oguchi
Computational Science Research Center
Hosei University
3-7-2, Kajino-cho, Koganei-shi, Tokyo 184-8584, JAPAN

Yoshifuru Saito
Department of Electrical & Electronic Engineering,
Hosei University
3-7-2, Kajino-cho, Koganei-shi, Tokyo 184-8584, JAPAN

ABSTRACT

Major applications of the wavelet transform have been focused on the waveform analysis and image data compression. One of the distinguished properties of the wavelet transform is that the major dominant factors can be extracted from the data. In the present paper, we apply this property to the vector data. As a result, we have succeeded in reducing the noisy vector data into noise free fine data. So, we apply this property to both ocean current data as time series and monthly-mean global wind data. This method of wavelet transform is suitable for the analysis of complex vector data.

KEYWORDS: Wavelet transform, Noise reduction, Vector data compression, Global wind field, Tidal current

1. INTRODUCTION

Major applications of the wavelet transform are both wave form analysis and image data compression (Saito,1996). One of the distinguished properties of the wavelet transform is extraction of major dominant factors from raw data. This method is available to analyze scalar data as a noise reduction method. In addition, the wavelet transform is suitable to compress data for transmission of the signal removing by the random noise. In the present paper, we try to apply this property to vector field of the environmental fluid and confirm to reduce the noisy vector data into noise free fine data (Matsuyama et al., 1997a, Matsuyama et al., 1997b).

Then, we apply this method to ocean current in oceanographical data and wind in meteorological data. The current and wind are mainly constituted from the periodic fluctuations and some random noise, so that these data are suitable to the application of the wavelet transform to compress the data by removing the noise.

2. METHOD OF VECTOR WAVELET TRANSFORM

Wavelet transform of the column vector, **X**, with order n of scalar element is generally expressed as

$$\mathbf{X}' = W\mathbf{X} \ , \tag{1}$$

where W is a n by n wavelet transform matrix, and $\mathbf{X}'$ is a wavelet spectrum. When the element of column vector $\mathbf{X}$ is two dimensional vector, $\mathbf{V}(\mathbf{V}_x,\mathbf{V}_y)$, the wavelet transform spectrum of $\mathbf{V}$ is composed by wavelet transform of each component and is expressed as

$$\begin{aligned} \mathbf{V}'_x &= W\mathbf{V}_x \ , \\ \mathbf{V}'_y &= W\mathbf{V}_y \ , \end{aligned} \tag{2}$$

where $\mathbf{V}'(\mathbf{V}'_x,\mathbf{V}'_y)$ is defined as transform spectrum of vector, $\mathbf{V}(\mathbf{V}_x,\mathbf{V}_y)$. Hereafter we call $\mathbf{V}$ *vector in column (VIC).*

Wavelet transform of matrix, M, is

$$S = W_m \cdot M \cdot W_n^{\,T} \ , \tag{3}$$

where S, M, W_m and W_n are the m by n wavelet, m by n original, m by m wavelet transform and n by n wavelet transformation matrices, respectively. When the element of matrix, M, is two dimensional vector, the wavelet transform spectrum is

composed by the wavelet transform of each component as well. Hereafter we call the matrix *vector in matrix (VIM).*

3. WAVELET TRANSFORM OF *VECTOR IN COLUMN (VIC)*

3.1 EXAMPLE OF MODEL VECTOR

First, we apply the method to a model *VIC* given by

$$V_i = \left(\sin\left(\frac{3\pi}{n} i\right), \cos\left(\frac{3\pi}{n} i\right) \right), i = 1,2,\cdots,n \quad , \qquad (4)$$

which contains a random noise vector having the magnitude between −1 and 1. Figure 1 shows the time series of the model vector with order n = 128. Figures 1(a), (b) and (c) are the vector calculated by Eq.(4), random noise vector, and model noisy vector, respectively. The vector wavelet transform is applied to the model noisy vector shown in Fig.1(c). The second-order Daubechies base function is employed for this wavelet transform. The calculated wavelet spectrum vector is shown in Fig.2 and demonstrates the nature of wavelet transform, i.e., concentration of the large magnitude vector near the mother wavelet. This result clarifies to be possible to compress the vector data as well as the scalar data.

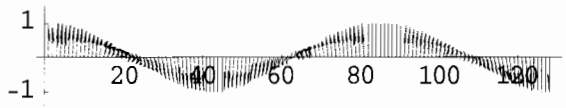

Fig.1(a) Vector data calculated by Eq.(4).

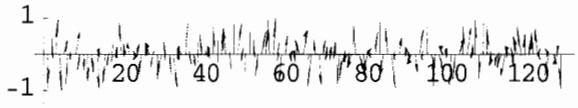

Fig.1(b) Random noise data for model vector data.

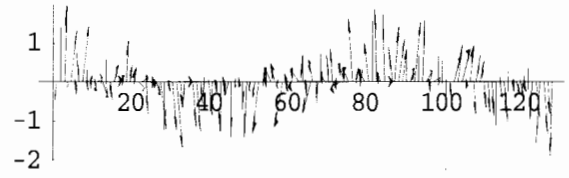

Fig.1(c) Model noisy vector data.

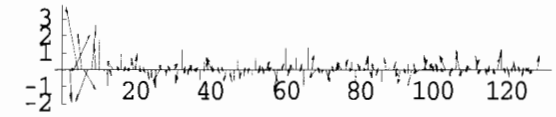

Fig.2 Wavelet spectrum vectors calculated by the second-order Daubechies base function.

Then we try to compress the vector data. In Fig.2, the wavelet spectra of only top 32 near the mother wavelet are adopted for calculation and the others are assumed to be zero, that is, the number of the calculated data is reduced into one-forth in comparison with that of the raw data. Figure 3 shows the vector data obtained by applying the inverse wavelet transform to the compressed data with the above method. In comparison with the raw vector data shown in Fig.1(c), it is fairly improved by the wavelet transform. In other word, the calculated vector data (Fig.3) are similar to the vector data shown in Fig.1(a), so the compression of the vector data by using the wavelet transform can decrease the noise in the raw data. Saito(1996) employed a correlation coefficient between the recovered and raw data in order to indicate the recoverability of data. The correlation coefficient of this method (recovery ratio) is 0.92, and it shows a good recovery.

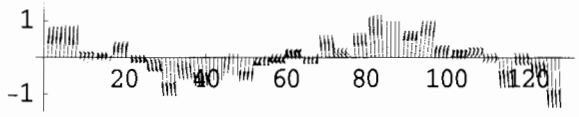

Fig.3 Vector data recovered from the top 32 shown in Fig.2.

The multiresolution analysis with wavelet transform decomposes the wavelet spectra (Fig.2) to the spectra at each level, and makes the inverse transform of each wavelet spectrum. After removing the high frequency levels by this analysis, the obtained vector series are shown in Fig.4. This shows that the time series are similar to those of vector in Fig.1(a). The recovery ratio between the results in Figs.4 and 1(a) is 0.92. Thus, this method is suitable to remove the random noise including in the basic data.

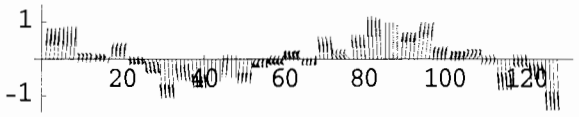

Fig.4 Vector data after removing high frequency level.

3.2 APPLICATION OF WAVELET TRANSFORM TO OCEAN CURRENT

For application to *VIC* data, ocean current data obtained at a station at the head of Suruga Bay, Japan, are used. The observed data are represented at every 10 minutes interval during the period from July 17 to 21, 1991. The number of data for analysis is 512. The main direction of the current is along the coastline, i.e., north-south direction. These data are suitable as *VIC* data. The dominant fluctuations are usually tidal frequencies such as diurnal and semidiurnal periods (Matsuyama 1991). The current data contain fluctuations of both the tidal and short periods (Fig.5). The short period

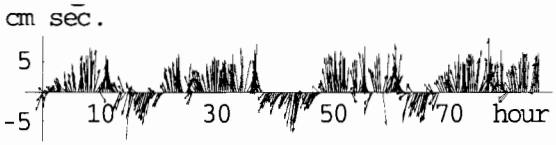

Fig.5 Time series of tidal currents at the head of Suruga Bay.

fluctuations are mainly random variations in relation to the oceanic turbulence which are considered as noise in this analysis. Figure 6 shows the result of the second-order Daubechies wavelet analysis of the current shown in Fig.5. The high current velocity is obviously concentrated near the mother wavelet. Figure 7 shows the time series of the current vectors by the inverse wavelet transform, using the top 128 spectra after removal of noise. The time series of the current vectors after the inverse wavelet transform (Fig.7) clearly indicate to be very similar to those of the raw data (Fig.5). These results express that main properties of the current vector in the time series record are kept by the inverse wavelet transform. The recovery ratio for reproduction is calculated as 0.94, i.e., the high correlation. Figure 8 shows the variations omitted in the data compression process. In this figure, the first 320 minutes variations are shown. The magnitude of the variation vectors has small in value and their vector direction take random.

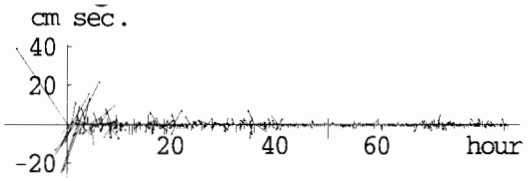

Fig.6 Wavelet spectrum vectors calculated by the second-order Daubechies base function.

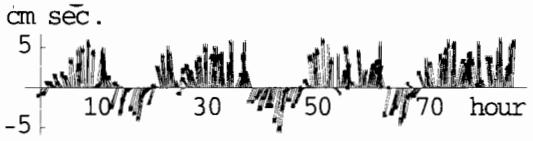

Fig.7 Tidal currents recovered from the top 128 shown in Fig.6.

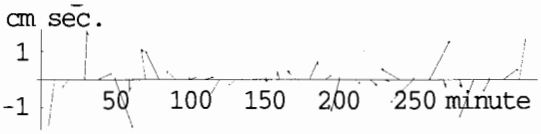

Fig.8 Time series of the currents omitted for the compression.

By means of the multiresolution analysis of the wavelet transform, the reproduced tidal current data for higher two level frequencies are small magnitude and their directions distribute at random. Therefore, these data may be regarded as the no major parts of all data. Figure 9 shows the time series of the tidal current removing the above high frequency parts, so that these are similar to the raw data. The recovery ratio between the results in Figs.7 and 9 is 0.94. Thus, the simple data compression makes it possible to reduce the noisy vector.

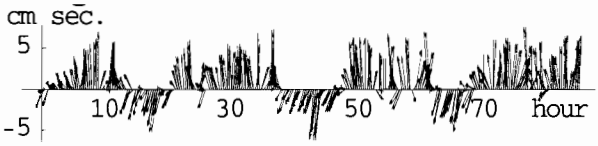

Fig.9 The tidal currents after removing high frequency level.

4. WAVELET TRANSFORM OF *VECTOR IN MATRIX (VIM)*

4.1 EXAMPLE OF MODEL VECTOR

We consider *VIM* data. The element vector, V_{ij} of m by n rectangular model matrix is expressed as follows

$$V_{ij} = \left(\sin\left(\frac{3\pi}{m} i\right), \cos\left(\frac{3\pi}{n} j\right) \right), \quad i = 1,2,\cdots,m,\ j = 1,2,\cdots,n \ . \tag{5}$$

In addition, the noise vector is made by random number between −1 to 1, as well. Figure 10 shows the model data, applying $m = 16 \cdot n = 32$ in Eq.(5). Figures 10(a), (b) and (c) are the vector data with no noise, random noise data, and model vector data including random noise, respectively.

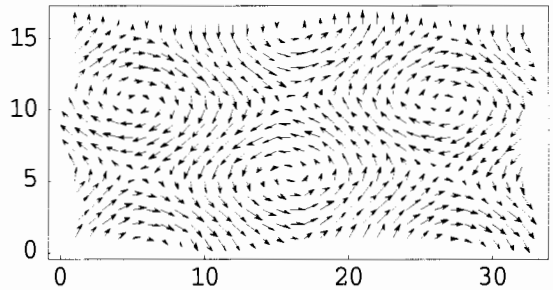

Fig.10(a) Vector data calculated by Eq.(5).

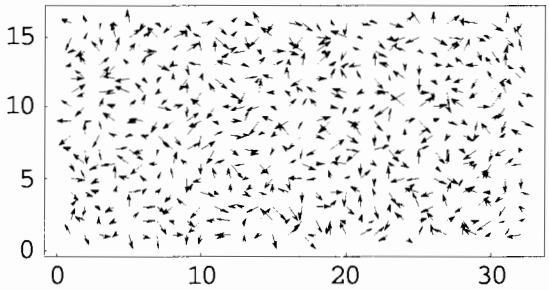

Fig.10(b) Random noise data for model vector data.

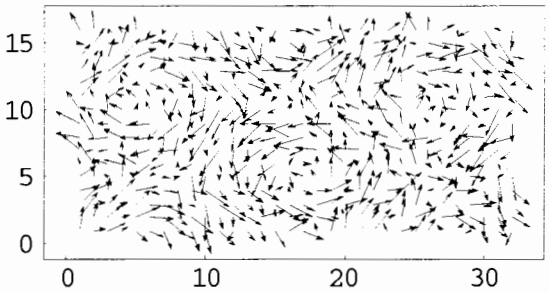

Fig.10(c) Vector data including the noise data.

Figure 11 shows the wavelet spectrum vector after transformation of the model *VIM* data shown in Fig.10(c) using second-order Daubechies base function. This result shows concentration of the major vectors near the mother wavelet, so it is possible to compress the *VIM* data with the same method as the scalar matrix. We examine to compress the *VIM*. The 8 by 16 part matrix near the mother wavelet in the wavelet spectrum is applied, and the other high frequency components are assumed to be zero in this inverse transformation. As a result, the number of data is reduced into one-forth compared with that the raw data. Figure 12 shows the recovered vector data by the inverse transformation of compressed spectra. The distribution of vectors significantly shows the suppression of the noise by the wavelet analysis, and therefore well agrees with that in Fig.10(a). The calculated recovery ratio between the

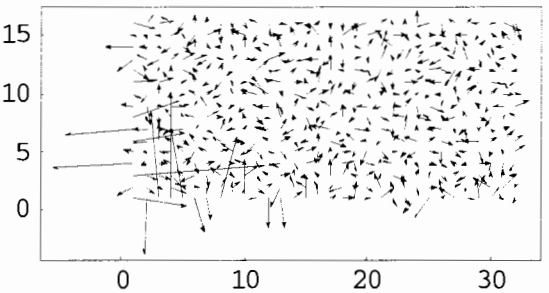

Fig.11 Wavelet spectrum vectors calculated by the second-order Daubechies base function.

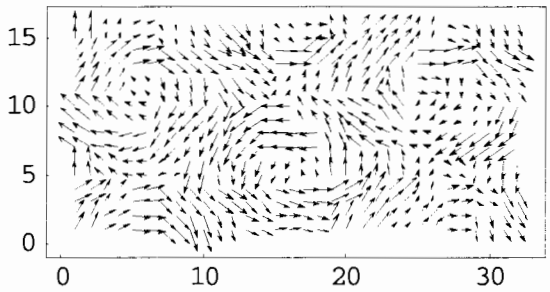

Fig.12 Vector data recovered from the top 8 × 16 shown in Fig.11.

vectors in Figs.12 and 10(a) is 0.90, so it indicates good reproduction of the data and is successful for data compression.

The multiresolution analysis of the wavelet transform gives the data by the inverse transform of the partial wavelet spectrum at each level. The analytical results show that the directions of vector at two levels in high frequency range are at random, so these levels may be composed of the noise. Figure 13 shows the inverse transformed vector after removal of the above two levels in high frequency range. The distribution of the vector in the figure is very similar to that in Fig.10(a), which is composed by the pure signal. The recovery ratio between the vectors in Figs.13 and 10(a) is 0.91, which is very high.

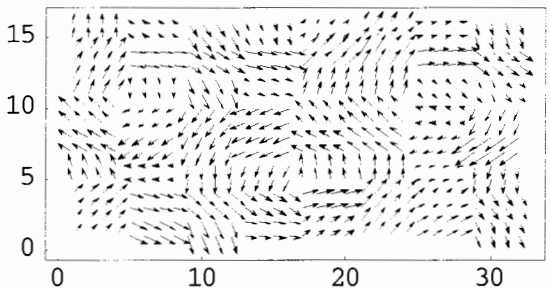

Fig.13 Vector data after removal of high frequency level.

4.2 APPLICATION OF WAVELET TRANSFORM TO THE WIND DATA

The horizontal distribution of the wind data is available for the application of the wavelet transform to vector fields. The data are NCEP/NCAR reanalysis ones with 2.5°× 2.5°grid size (longitude × latitude). Figures 14 and 15 show the monthly mean winds at 250-hPa surface on July 1993 and July 1994, respectively. The former was very lower temperature than the average in summer in Japan, while the latter was very high temperature than the average in Japan. The characteristics of the eastward strong wind around the Japan, i.e., the Jet Stream, located the south (37•to 47•N) in 1993's summer and the north (42•to 52•N) in 1994's summer in comparison with

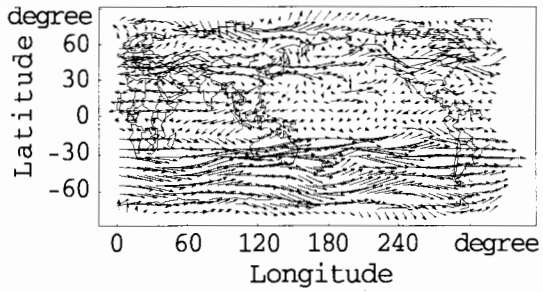

Fig.14 Monthly mean wind data on July 1993.

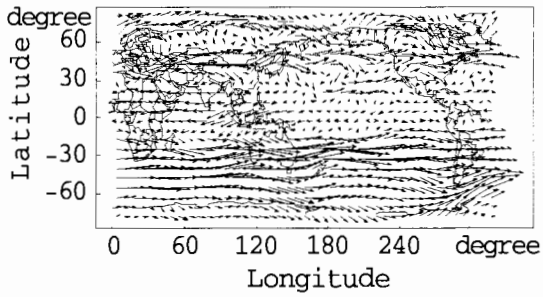

Fig.15 Monthly mean wind data on July 1994.

the mean location. The number of data is 64 × 128, so the studying region is not the whole earth , but is limited from 75•S to 82.5•N and 0•E to 42.5•W. In order to show clearly the difference of the Jet Stream in both years, Figures 16 and 17 show the wind distributions around Japan in detail. In July, the

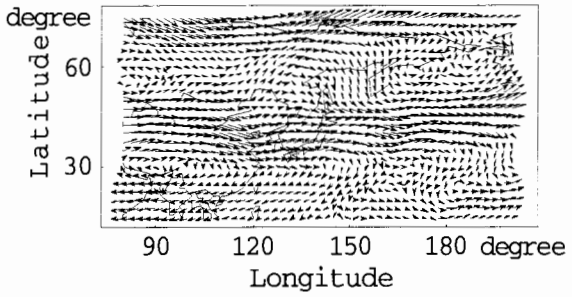

Fig.16 Monthly mean wind data around Japan on July 1993.

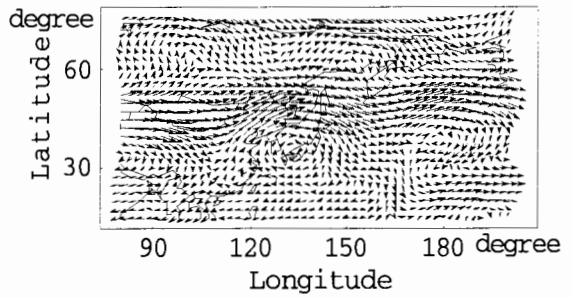

Fig.17 Monthly mean wind data around Japan on July 1994.

mean speed of the Jet Stream is about 30m/s in Northern Hemisphere, while it is 40 to 50m/s in Southern Hemisphere in winter.

Figure 18 shows the wavelet spectra of wind calculated under the second-order Daubechies base function. It is recognized that the high velocity vectors gather near the mother wavelet. Figure 19 shows the dominant wind vector field extracted from the top 32 × 64 region in Fig.18. The global wind field is very similar to that by the raw data shown in Fig.16. Thus, *VIM* fields are reproduced by the wavelet transform method as well. The recovery ratio is 0.99 which means excellent reproductivity. The omitted noise vector data by compression are shown in Fig.20, and their magnitudes are about one-tenth smaller than those of the vector shown in Fig.19. In addition, the direction of the vector is at random (Fig.20). The wind vector, which is reproduced by the inverse transformation of the higher two level frequencies, is shown in Fig.21. The wind data are small in magnitude and at random in direction as well. Figure 22 shows the wind vector after removal of the noise data. Its distribution is very similar to the raw data shown in Fig.16, and therefore, the recovery ratio is 0.99. These are the results in July 1993, and these are the same characteristic in July 1994 as well.

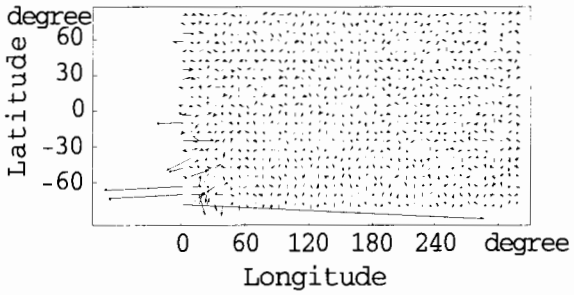

Fig.18 Wavelet spectrum vectors are calculated by the second-order Daubechies base function.

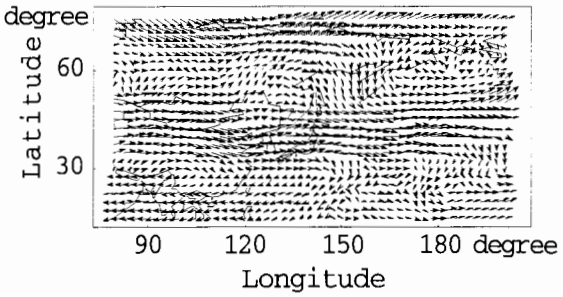

Fig.19 Wind vectors recovered from the top 32 × 64 region shown in Fig.18.

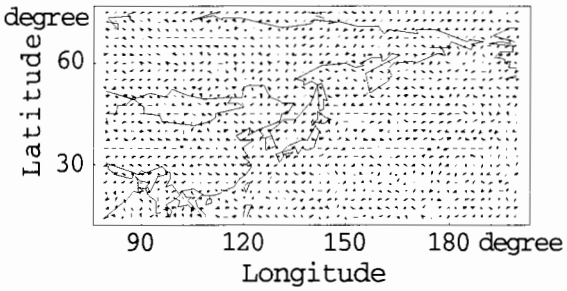

Fig.20 Wind vectors omitted for the compression.

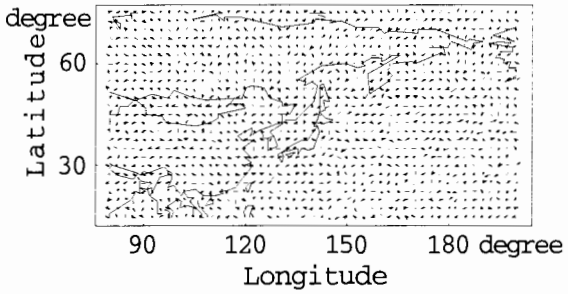

Fig.21 Wind vectors of the high frequency level on July 1993.

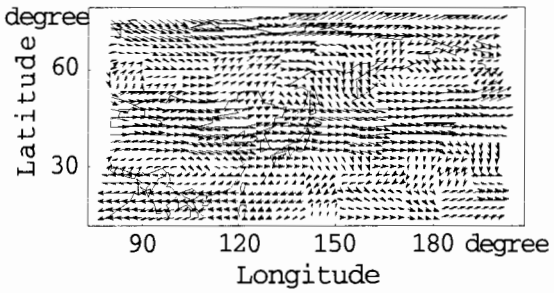

Fig.22 Wind vectors after removal of high frequency level on July 1993.

5. SUMMARY

As shown above, through the wavelet transform method, we can present the extraction of the dominant frequency or wave number from such observational vector fields as the velocity in ocean and atmosphere. This method compresses the data effectively, so it is suitable to transmission of vast amounts of vector data such as the wind and current.

ACKNOWLEDGMENTS

The authors would like to thank Prof. M. Matsuyama in Tokyo University of Fisheries and the late Prof. T. Nitta in Center of Climate System Research, the University of Tokyo to supply the current and wind data.

REFERENCE

Matsuyama, M.,1991 "Internal Tides in Uchiura Bay", in *Tidal Hydrodynamics (ed. by B.Parker)*, 489-503. Jhon Wiley & Sons, INC. New York.

Matsuyama,S., Oguchi,Y., and Saito,Y., 1997, "Applications of the Wavelet Analysis of the Vector Data," *Proceedings of the Conference on Computational Engineering and Science*, Vol.2, No.2, 375-378 (in Japanese).

Matsuyama,S., Oguchi,Y., and Saito,Y., 1997, "Applications of the Wavelet Transformation to the Meteorological Data," *Proceedings of the Conference on Computational Engineering and Science,* Vol.2, No.2, 359-362 (in Japanese).

Saito,Y., 1996, "Wavelet Transform using Mathematica," Asakura-shoten Ltd., Tokyo (in Japanese).